

DEVELOPMENT OF A 480-640 GHz TUNERLESS SIS MIXER FOR FIRST HIFI/BAND 1

M. Salez¹, Y. Delorme¹, I. Péron^{1,2}, F. Dauplay¹, B. Lecomte¹, M.-H. Chung^{1,4}, J. Spatazza³, M. Guillon¹, K. Schuster², J.-M. Krieg¹, A. Deschamps¹

¹DEMIRM, Observatoire de Paris, 77 avenue Denfert-Rochereau, 75014 Paris, France

²IRAM, Domaine universitaire de Grenoble, 300 rue de la piscine, 38406 Saint-Martin d'Hères, France

³CNRS-INSU, Division Technique, 1 place Aristide Briand, 92195 Meudon, France

⁴Taeduk Radio Astronomy Observatory, San 36-1, Whaam-dong, Yusong-gu, Taelon 305-348, South Korea

ABSTRACT

This paper describes the current work at DEMIRM and IRAM to meet the bandwidth-sensitivity specifications of the HIFI Band 1 instrument (480 – 640 GHz). A specific design philosophy was implemented to optimize this Nb-based SIS mixer. We came to design a new tunerless mixer mount, simplified in terms of fabrication and optimized for a 30% bandwidth. It incorporates a high-efficiency electromagnet which can provide several flux quanta to the junction with less than 10 mA. A novel high current density junction fabrication process was set up at IRAM for this project, using negative resist e-beam lithography. Preliminary results based on Fourier Transform Spectroscopy measurements and heterodyne calibrations are presented and discussed. So far, mixer noise values (corrected for the optics) of respectively 65 K and 140 K were measured with a first batch of junctions with a current density of 10 kA/cm². More recently, with a new batch of higher current density junctions, receiver noise values (double sideband, uncorrected) of 130 K were measured at some frequencies.

1. INTRODUCTION

Both a very large bandwidth (about 30 %) and a high sensitivity (3 times the quantum limit or less) is required from the Band 1 (480-640 GHz) mixer unit of HIFI, the heterodyne instrument aboard ESA's cornerstone Herschel Space Observatory (formerly FIRST) satellite, scheduled for launch in 2007 [1]. HIFI comprises several SIS and HEB mixers covering a wide range of frequencies through several adjacent bands. Band 1 will consist of two identical tunerless waveguide mixers, with corrugated feedhorns, respectively sensitive to both perpendicular polarizations. The intermediate frequency must cover a 4 to 8 GHz bandwidth with a very low level of ripple (3 dB). The State of the Art (resp. Goal) performance for Band 1 is a linear interpolation between 80 K (resp. 70 K) DSB at 480 GHz and 130 K (resp. 110 K) DSB at 640 GHz. However, achieving a bandwidth of 30% with an SIS mixer is a challenge, and the so-called SOAP truly remains, to this day, a goal yet to be achieved. In addition, the SIS mixers of HIFI must be space qualified, and must satisfy a number of constraints, in terms of mass, volume, power dissipation, EM shielding, which impact on their design.

2. TUNERLESS WAVEGUIDE MOUNT

Since we aim at a large bandwidth mixer, it is essential that input and output impedances of every component of the mixer be well defined. In particular, the embedding impedance of the waveguide mount at the location of the substrate must be well known (and possibly tuned)

over the 480 – 640 GHz, since it must be matched to the SIS device by means of an integrated microstrip circuit. Obviously, the job of conjugate-matching several mixer passive components would be nicer if all the impedances stayed constant within the frequency range of interest, with as little reactive part as possible. From this standpoint, resonant elements such as integrated tuning stubs and waveguide backshorts should be used scarcely, and probably the best ‘tunerless’ mixer is one with no such tuner at all.

Therefore we have left aside some commonly made assumptions on waveguide mixer embedding impedances and best tunerless waveguide mount geometries — demonstrated by excellent results in several groups [2,3], to carry out extensive EM simulations of a waveguide mixer varying many of its parameters, including the shape of the bow-tie antenna and the first sections of RF choke filter [4]. This was done using a 3D software package [5] allowing to explore, in particular, the influence of the quartz substrate inserted across a reduced-height rectangular waveguide, and the effect of positioning errors and mechanical tolerances. We found the substrate orientation to have a major influence, and we could optimize the geometry in order to provide a nearly frequency-independent and imaginary-part free impedance, close to 70Ω , to the bow tie center where the SIS circuit is located. Figure 1 shows the calculated evolution of this impedance with backshort location. It is important to note that our simulations have also confirmed some earlier results published by other groups, while this optimum embedding impedance corresponds to a particular substrate orientation and backshort location. The 50 μm -thick quartz substrate has to be mounted with the metallization looking away from the input waveguide, and facing the backshort another 50 μm above it, flush with the top of the substrate channel. This makes the fabrication of tunerless waveguide mixers much easier, since no micromachining of a backshort-terminated waveguide is required.

3. SIS CIRCUIT DESIGN

Following a similar strategy, the SIS junction parameters and the integrated RF microstrip circuit geometry have also been optimized to provide a wide-band match to the mixer mount embedding impedance. The most convenient type of circuit consists of an end-loaded single junction circuit (baseline), in which a two-section Tchebychev impedance transformer is designed so as to stretch the RF coupling bandwidth. This solution requires high current density (typically $15 \text{ kA}/\text{cm}^2$) SIS junctions. Another approach, more complex because of the advent of Josephson currents, is the use of parallel arrays of junctions (fall-back option).

Regardless of the type of SIS circuits, optimizing them was done in three consecutive stages: first, the electrical lengths and characteristic impedances of every section of the SIS circuit were optimized using HP Libra. This allowed us to rapidly optimize circuits with a large number of degrees of freedom and to investigate the expected yield. We plugged into the commercial software all the fabrication tolerances and maximum errors associated to all parameters, and did a statistical analysis, leading us to select our circuit designs not on the sole basis of optimum result but also of optimum yield.

In a second stage, the sets of electrical lengths and characteristic impedances were converted into real microstrip circuit dimensions using the theory of superconductive microstrip transmission lines.

To verify the circuit design, the noise performance to expect from any optimized circuit — placed in our tunerless waveguide mount — was calculated at any frequency and for various LO powers and bias voltages, using a numerical code written in C++ using Tucker formalism of quantum mixing in the 3-port approximation. From these predictions, it became clear (see Fig. 2) that achieving the RF bandwidth specified for Band 1 with a ‘flat’ receiver noise would be an extremely difficult task using a single junction design and Nb/AlOx/Nb

technology. However, twin-parallel and multi-junction arrays ($N > 2$), as first proposed by NRO [6] should allow to meet the goals. Our own proposed multi-junction array geometries, using non-uniform spacings between SIS junctions, were presented earlier [7].

4. SIS JUNCTION FABRICATION

Considering the maximum RF frequency we need and the degrees of maturity and reliability of various SIS technologies, for current densities up to 15 kA/cm^2 Nb/AlOx/Nb junctions in association with Nb/SiO₂/Nb microstrip circuits appear as the best choice materials for the mixers of HIFI/Band 1.

High-current density (15-kA/cm^2) SIS junctions with areas of $1 \text{ }\mu\text{m}^2$ or smaller are required to avoid shunting by the tunnel barrier capacitance in high frequency applications. Because the standard SIS fabrication process in use at IRAM — UV360 contact lithography — is limited in precision for the definition of junctions smaller than $2 \text{ }\mu\text{m}^2$, a new fabrication process using e-beam lithography for the definition of the HIFI/Band 1 junctions was developed [8]. To make it compatible with the existing process, a mix & match process was chosen, where the same negative resist layer can be both e-beam and UV-exposed to produce self-aligned structures for either the junctions pattern or the larger contact areas. As shown in Fig.3, this process involves less steps than positive e-beam lithography. More details on the fabrication process can be found in [8]. Out of 80 junctions measured, 57% of them displayed good I-V curves with $R_{\text{subgap}}/R_n > 20$. The results show that despite earlier claims it is possible to fabricate high quality Nb-Al-AlOx-Nb junctions with current densities well above 10 kA/cm^2 with good yield.

The trilayer consists of a 120 nm niobium (Nb1) bottom electrode, a 10 nm Al layer oxidized in pure oxygen at room temperature, and 60 nm niobium (Nb2). The RF microstrip circuits share the same Nb1 bottom electrode with the trilayer, and use a 200 nm thick dielectric layer (SiO₂) and a 430 nm niobium counter-electrode (Nb3). Figure 4 shows a micrograph of a circuit.

5. PRELIMINARY MEASUREMENTS

Fourier Transform Spectroscopy (FTS) measurements and heterodyne hot/cold load calibrations were done with the first SIS circuits produced by IRAM. For the heterodyne tests we made a prototype tunerless waveguide mount, simple—for instance with a plain diagonal horn and a massive conventional superconducting magnet—yet with the substrate positioning and the backshort location found to be optimum from our 3D simulations. We adopted this solution to make rapid validations of the circuits and we expect the next waveguide mount to be of much better quality.

Figure 5 shows on the same plot the FTS response of one such circuit (10 kA/cm^2) both mounted in an open structure (prior to dicing of the individual chips) and mounted in the waveguide mount. Several things must be noted. First, the envelopes of both FTS responses are quite similar. This demonstrates that the new tunerless mixer mount is nearly 'transparent' impedance-wise. Indeed, the source impedance seen by the SIS circuit in the open-structure case is close to $100 \text{ }\Omega$ over most of the band, not too different from the $\sim 70 \text{ }\Omega$ waveguide mixer environment. With either type of feed, therefore, the computed RF coupling response is dominated by the complex admittance of the SIS circuit itself.

Second, the measured response of the single-junction circuit agrees with the simulations: the 'twin-peaks' like curve is mainly due to the Tchebychev circuit, designed for the widest band possible. This shows the limitations of the microstrip transformer approach

for a 30 % relative bandwidth, since it results, as shown in Fig. 6, in an increase of the receiver noise in the center of the band mirroring the decrease of RF coupling. However, the good agreement between measurements and simulations is encouraging and validates our choice of strategy. In particular, the fact that the 480-640 GHz bandwidth has been obtained from the very first batch of junctions seems to validate our 'best-yield design' approach and the reliability of the new junction fabrication process. The best receiver noise measured for one device always occurs at two frequencies where the RF coupling and the mixer gain peak. An example of these noise values is given in the Table I below, also providing a correction for the optics losses. The influence of the latter was quantified using FTS measurements of refractive indices and absorption coefficients of the optical components at all frequencies (Table II). The calculations assumed a 7 K IF noise and included the contribution of zero-point field fluctuations to the noise, at temperature T_i and frequency ν :

$$T_i \longrightarrow T_{i,ZPF} = \frac{h\nu}{2k_B} \cdot \coth\left|\frac{h\nu}{2k_B T_i}\right|$$

With another device at 15 kA/cm², and after removing some optical components (the 3.4-mm thick rexolite lens and one IR filter) in the cryostat we could measure a receiver noise temperature of 130 K around 530 GHz (see fig. 7).

Table I

Frequency (GHz)	T _{rec, uncor} (K)	T _{RF} (K)	G _{RF}	T _{rec, cor} (K)	T _{rec sim} (K)
480	280	95.2	0.35	65	60
610	500	73	0.33	141	87

Table II

Component	Material	Thickness (mm)	Index n	Absorption $\alpha(\text{cm}^{-1})$	Power Transmission
Beam splitter	Mylar	0.009	1.732	0.74	0.97
Vacuum window	Mylar	0.025	1.732	0.74	0.85
Filter 4.2 K	Fluorogold	0.508	1.654-1.657	1.6-2.8	0.74
Lens 4.2 K	Rexolite	3.4	1.6	0.55	0.6

6. LOW-CURRENT ELECTROMAGNET

SIS mixers require the application of a magnetic field in the tunnel barrier plane to null the DC average of Josephson currents. This is commonly achieved with a superconducting electromagnet. In the case of HIFI, the low maximum current allowed—for thermal dissipation reasons—imposes the design of a highly efficient electromagnet, able to provide a few magnetic flux quanta in the SIS junction for a maximum current of 10 mA.

Figure 8 shows the proposed electromagnet for the Band 1 mixers. It consists of a pair of symmetrical electromagnets: the cores are made out of a high magnetic permeability material, coiled with hundreds of turns of NbTi/Cu 100-micron gauge wire, and the polar pieces reach the plane of the SIS substrate. A prototype electromagnet using cryoperm was made and measured at room temperature and 4.2 K. The cryoperm material was provided by Ammuneal Corp [9] then bent into shape and thermally processed [10]. The prototype was

winded in house by hand with 1100 turns of 120-micron formvar-insulated copper wire, then characterized using a Hall probe.

At room temperature, the magnetic field produced by the magnet saturates between 900 and 1100 Gauss, depending on the size of the gap between the polar pieces (~1 mm typ.). As expected, the saturation field, reached for about 150 mA (see Fig. 9), is larger at 4.2 K than at 300 K. These saturation levels are lower than the ~8000 Gauss specified for the bulk cryoperm material, nevertheless sufficient for our application. The magnetic permeability does not vary with temperature, and no hysteresis was noted. These measurements ensure that the electromagnet designed for Band 1 will meet the HIFI specs, providing 300 Gauss — inducing more than 3 flux quanta in a one-micron-square SIS junction — with only 10 mA.

7. DEMONSTRATION MODEL MIXER

Figure 10 shows an Autocad view of the Demonstration Model (DM) mixer for Band 1, as currently designed.

The most important feature for our wideband coupling design is the orientation of the substrate, which lies on the feedhorn section of the mixer. The substrate is surrounded by a set of printed boards supporting various functions: IF output line (with or without an IF impedance transformer) with DC block; grounding of the SIS device with an integrated heater to get rid of occasionally trapped flux; DC bias circuit with filters. These must be highly efficient in the microwave region, to provide an isolation better than 30 dB and protect the SIS device from EMI/ESD. We propose the use of distributed planar RC filters using lossy suspended striplines. The resistor is a thin TaN film and the dielectric is Ta₂O₅N. These novel filters are attractive because of their smallness and because they will efficiently reject any high frequency noise above a certain cutoff frequency (e.g. 50 MHz), whereas their lumped equivalents provide less rejection and have resonances in the microwave range. We will report on the performance of the filters elsewhere.

Corrugated feedhorns for the DM have been designed (in concertation with the other HIFI mixer designers, for the sake of standardization between bands) and are now fabricated: the mandrels were machined by Société Audoise de Précision [11] out of aluminum 7175; electrodeposition of 24-carat gold—to avoid voids—and copper on the mandrels is done at Protection des Métaux [12]. We will investigate their beam quality (E and H symmetry, sidelobes, crosspolarization, return loss) by amplitude and phase measurements at IRAM. Figure 11 shows the calculated beam pattern and Fig. 12 shows EBM photographs of 70-micron and 20-micron wide corrugations (on a feasibility study prototype).

8. CONCLUSION

We have designed a mixer for HIFI/ Band 1, which we are currently validating by FTS and heterodyne measurements. The Demonstration Model of this mixer will be partially functional (some points at the SOAP specs within the band) and fully compliant with the interface specifications (dimensions, mass and power dissipation budget, ranges of voltages and currents, LO power required). In particular, the DM will include several items which have been specially developed for this project: a high efficiency electromagnet with a cryoperm core, high current density Nb junctions processed by e-beam lithography, and a corrugated feedhorn. We demonstrated with FTS measurements that the waveguide mount needs no fixed length of backshort to provide a wide bandwidth, hence greatly simplifying the manufacture of the mounts. To improve the receiver sensitivity across the band in later deliveries

(upgraded DM or QM, FM), new SIS circuits will be required, including non-uniform parallel arrays of junctions, a development currently in progress at DEMIRM.

ACKNOWLEDGEMENTS

We thank, for financially supporting the project and Frédéric Dauplay, the Centre National d'Etudes Spatiales and CNRS, the Institut National des Sciences de l'Univers (INSU). We are grateful to Pascal. Fèbvre and Frédéric Garet of Université de Savoie for the measurements of materials at submm wavelengths. We wish to thank Karl Jacobs, Netty Honingh, Gert De Lange, Hans Golstein, and Jaap Evers for open and helpful discussions. We thank for their support Jean-Pierre Ayache, and Raoul Entringer of INSU's Division Technique in Meudon. The feedhorns beam pattern measurements are to be performed at IRAM by Matt Carter.

REFERENCES

- 1 H. v.d. Stadt, G. Beaudin, T. De Graauw, K. Jacobs, and N. Whyborn, 'Detectors for the heterodyne spectrometer of FIRST', *Proc. of the ESA Symposium 'The Far Infrared and Submm Universe'*, 457, IRAM, Grenoble, France, April 15-17, 1997.
- 2 J.Kooi et al., 1994, '180-425 GHz low noise SIS waveguide receivers employing tuned Nb/AlOx/Nb tunnel junctions', *International J. of Infrared and Millimeter Waves*, **15**, 5, 783.
- 3 C.-Y. Tong, R. Blundell et al., 'A fixed tuned low noise SIS receiver for the 600 GHz frequency band', *Proc. 6th International Symposium on Space Terahertz Technology*, 295, Pasadena, 1995.
- 4 Microwave Studio, Computer Simulation Technology, <http://www.cst.de>
- 5 M. Salez, Y. Delorme, F. Dauplay, B. Marchand, B. Lecomte, and M.-H. Chung, 'Design of a fixed-tuned 30% bandwidth SIS receiver for FIRST/HIFI Band 1 (480-640 GHz) and other space applications', *Proc. 4th European Workshop on Low-Temperature Electronics, WOLTE-4*, ESTEC, Noordwijk, NL, June 21-23, 2000.
- 6 S.-C. Shi, T. Nogushi, and J. Inatani, 'Analysis of the bandwidth performance of SIS mixers with distributed junction arrays', *Proc. 8th International Symposium on Space Terahertz Technology*, p.81, Harvard University, MA, March 25-27, 1997.
- 7 M. Salez, Y. Delorme, M.-H. Chung, and F. Dauplay, 'Simulated performance of multijunction parallel array SIS mixers for ultra broadband submillimeter-wave applications', *Proc. 11th International Symposium on Space Terahertz Technology*, pp. 343-358, Ann Arbor, MI, May 1-3, 2000.
- 8 I. Péron, P. Pasturel, and K.-F. Schuster, 'Fabrication of SIS junctions for space borne submillimeter wave mixers using negative resist e-beam lithography', *Proc. of the Applied Superconductivity Conference, ASC'00*, Virginia Beach, Sept. 17-23, 2000.
- 9 Amuneal Corp, 4737 Darrah Str., Philadelphia, PA 1924-2705; larrym@amuneal.com.
- 10 Division Technique INSU, place Aristide Briand, 92195 Meudon, France; *Bodycote Hit*, 25 rue Louis Ampère, Z.I. des Chanoux, 93330 Neuilly-sur-Marne, France.
- 11 Société Audoise de Précision, Z.A. du Pont, F-81500 Ambres, France.
- 12 Protection des Métaux, 57-59 rue de Saint-Mandé, 93511 Montreuil, France.

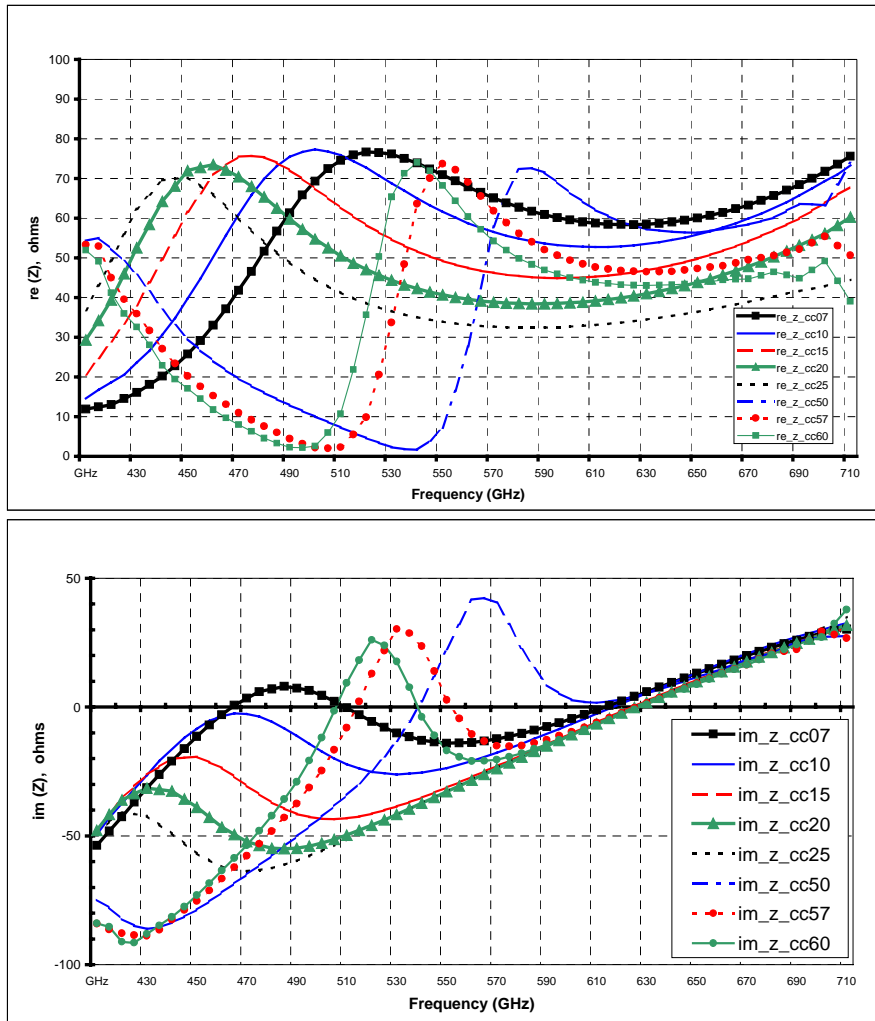


Figure 1. Real and imaginary parts of the waveguide mount embedding impedance seen at the center of the bow-tie probe, simulated for different waveguide backshort locations (distance of backshort from metallization is expressed in the legends in percents of the guided wavelength).

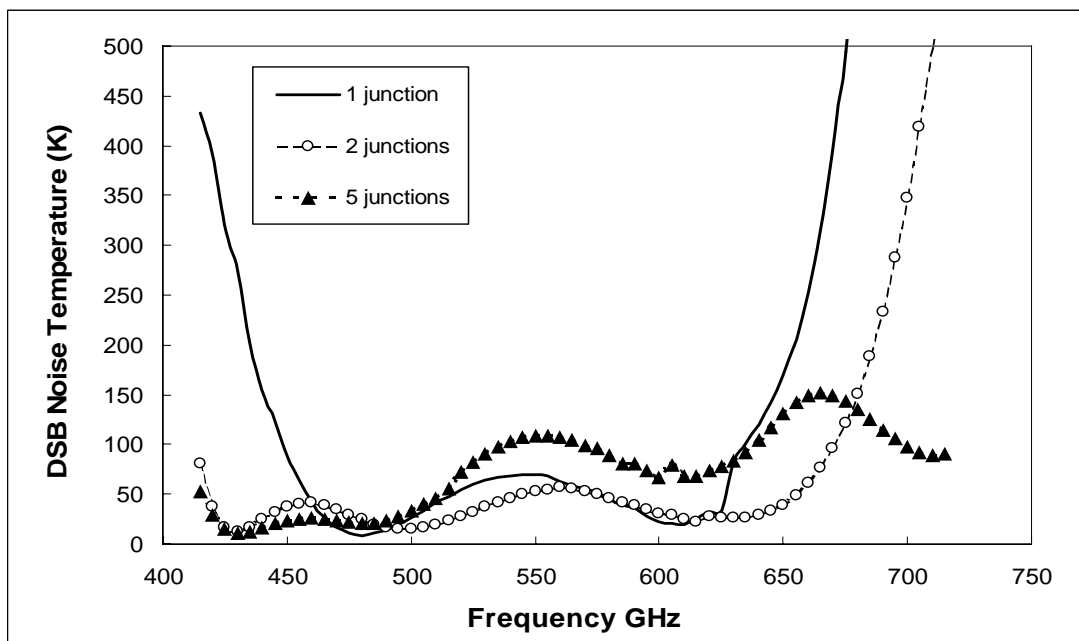


Figure 2. Predicted DSB mixer noise performance for a single-junction, twin-parallel junction, and $N=5$ junction array mixers optimized for Band 1.

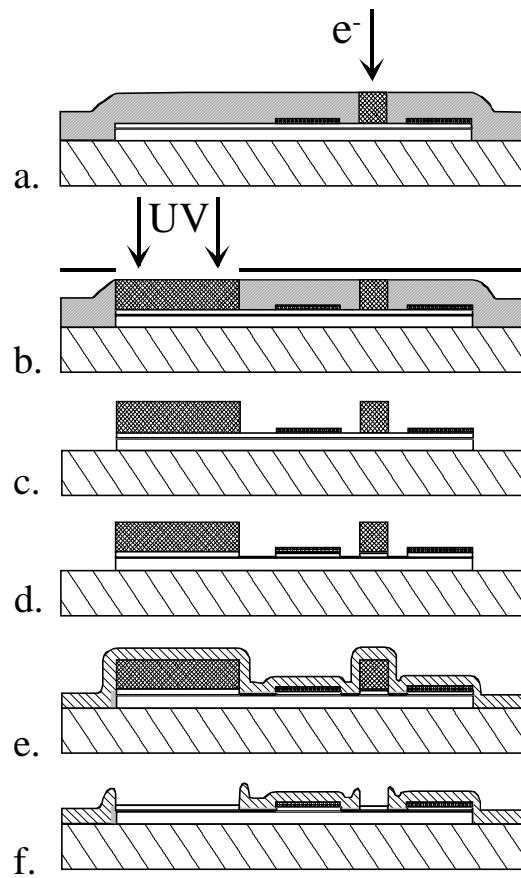


Figure 3. Schematic of the mix & match process: a. e-beam lithography junction definition; b. contact area UV-mask aligner lithography; c. junction and contact pattern after development; d. reactive ion etching of Nb₂; e. SiO₂ deposition; f. SiO₂ liftoff.

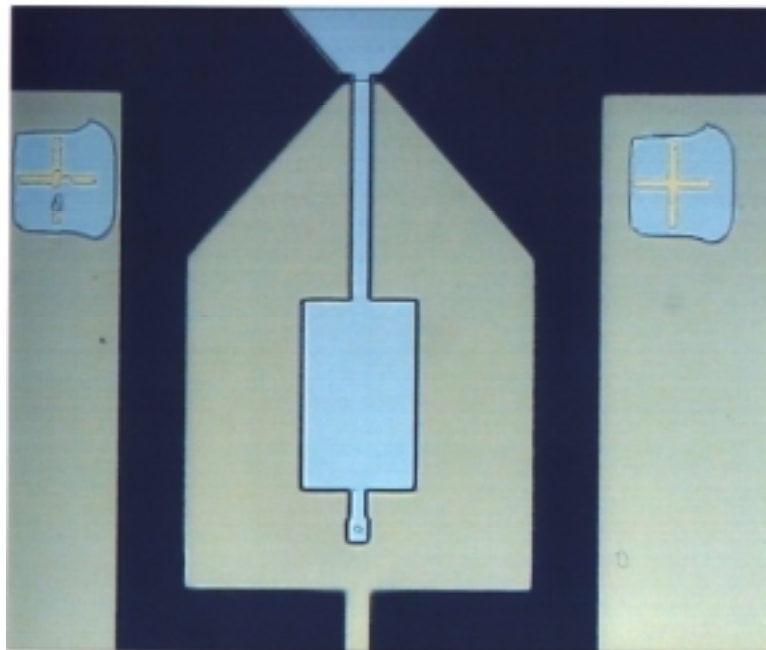
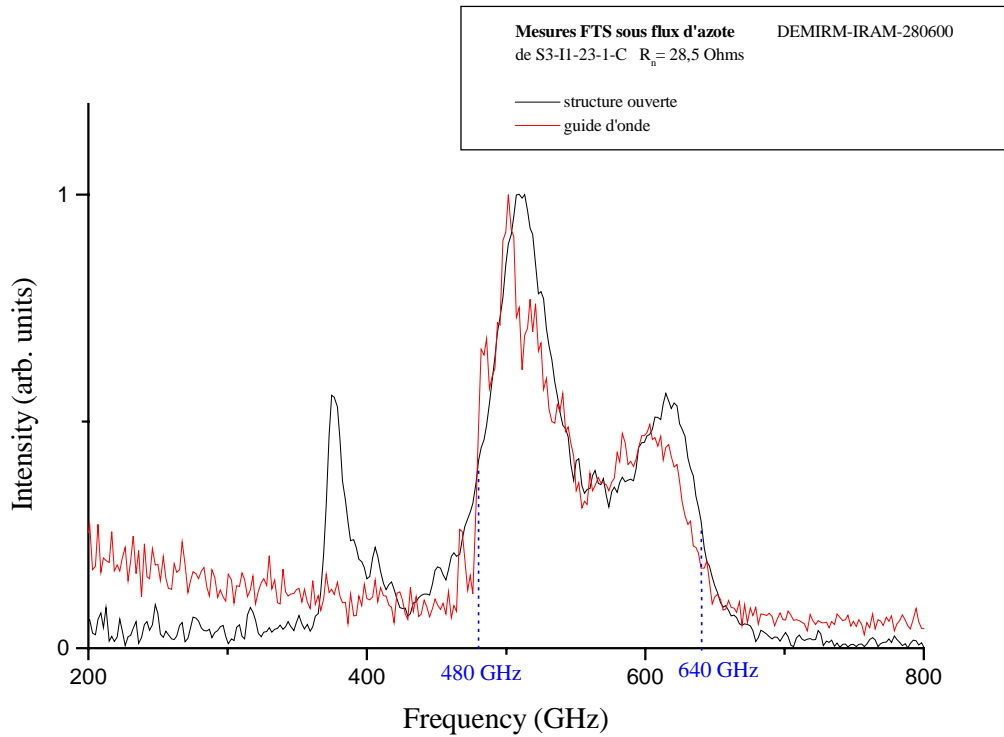


Figure 4. Photograph of a 1- μm^2 junction defined by EBL with the new IRAM process.

(a)



(b)

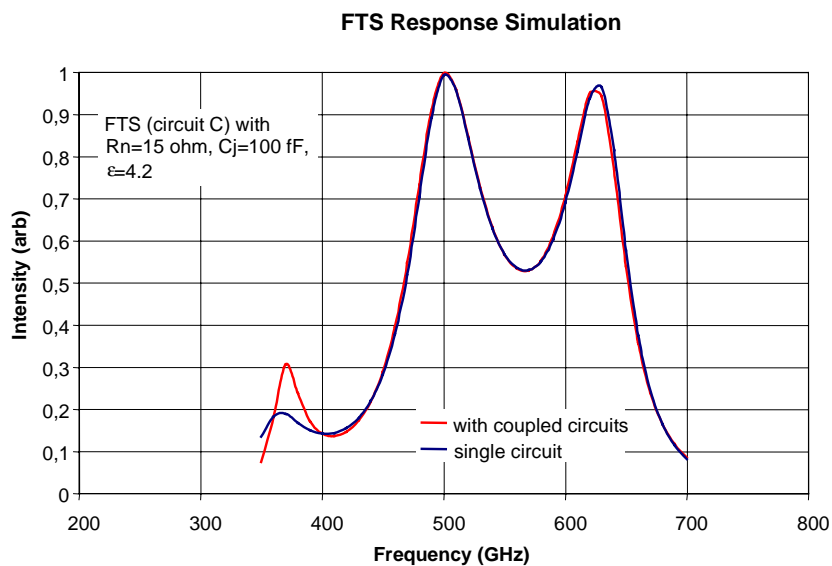


Figure 5. (a) FTS response of a $1 \mu\text{m}^2$, 10 kA/cm^2 Nb/ AlO_x /Nb junction with a Tchebychev transformer (device # S3-I1-23-1-C), coupled to the radiation both quasioptically and in the tunerless waveguide mount. (b) Simulated FTS response: we showed the peak at 380 GHz in the open structure measurement to be a mere consequence of radiation coupling to the nearby devices on the undiced chip.

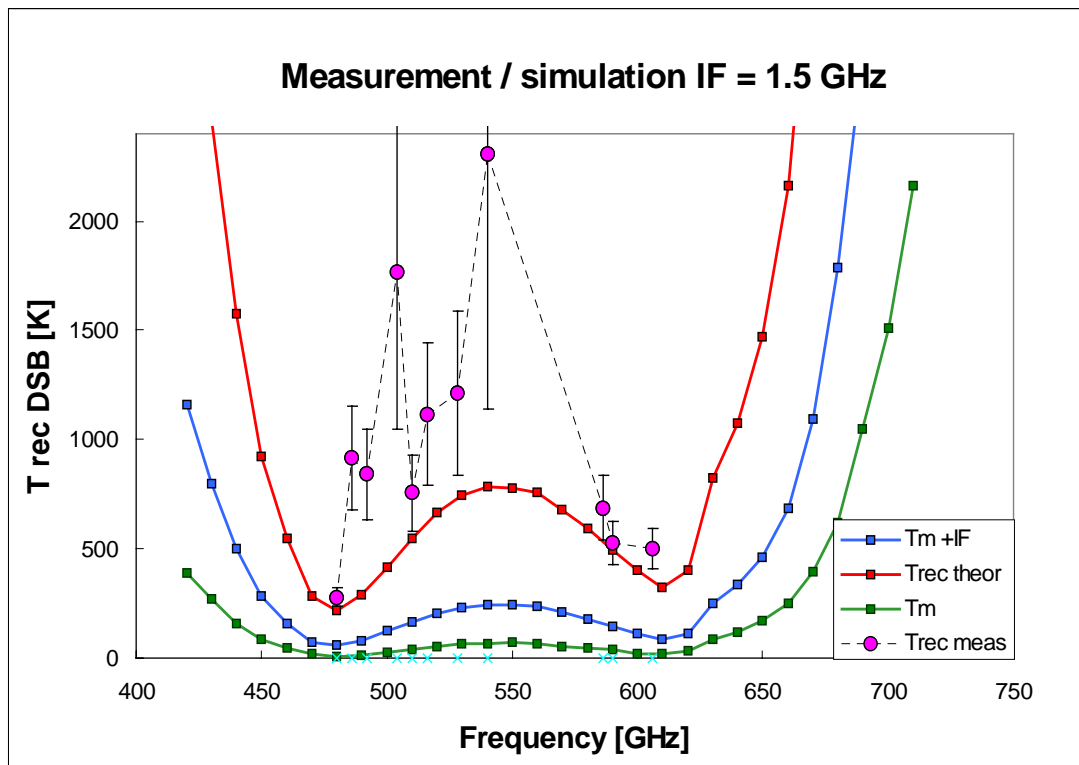


Figure 6. Comparison of heterodyne calibration with simulated DSB noise performance. The calculated noise was optimized (w.r.t. LO power, bias voltage) and includes a 7 K IF system noise at 1.5 GHz. The RF noise contribution was computed after measurements from 100 to 1500 GHz of the refractive index and absorption coefficient of all optical materials used in the experiment. No data is available on this plot below 480 GHz nor above 610 GHz for lack of LO source.

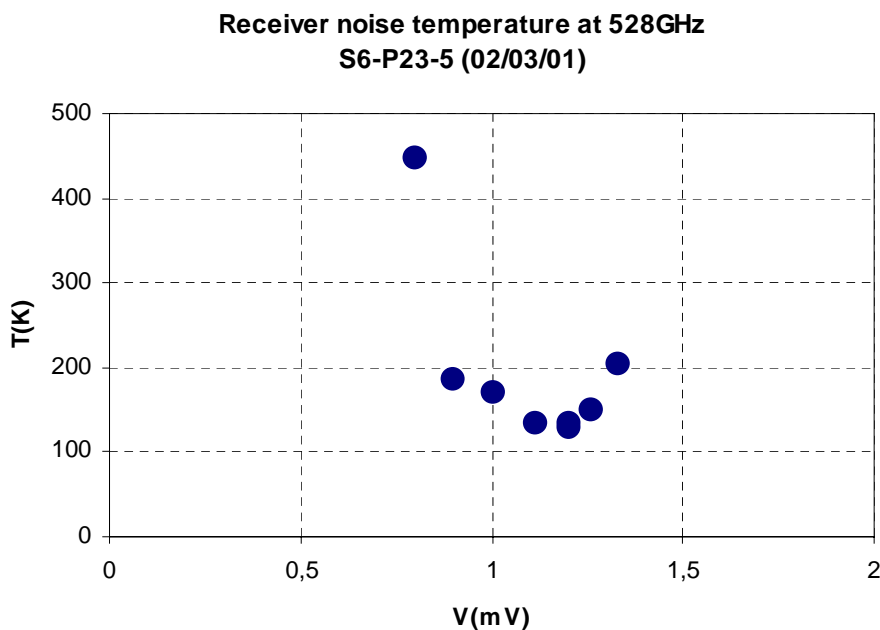


Figure 7. Measured receiver noise temperature versus bias voltage at 528 GHz for device # S6-P23-5 (15 kA/cm^2).



Figure 8. One half of the cryoperm electromagnet designed for Band 1 (1100 turns); artist's view.

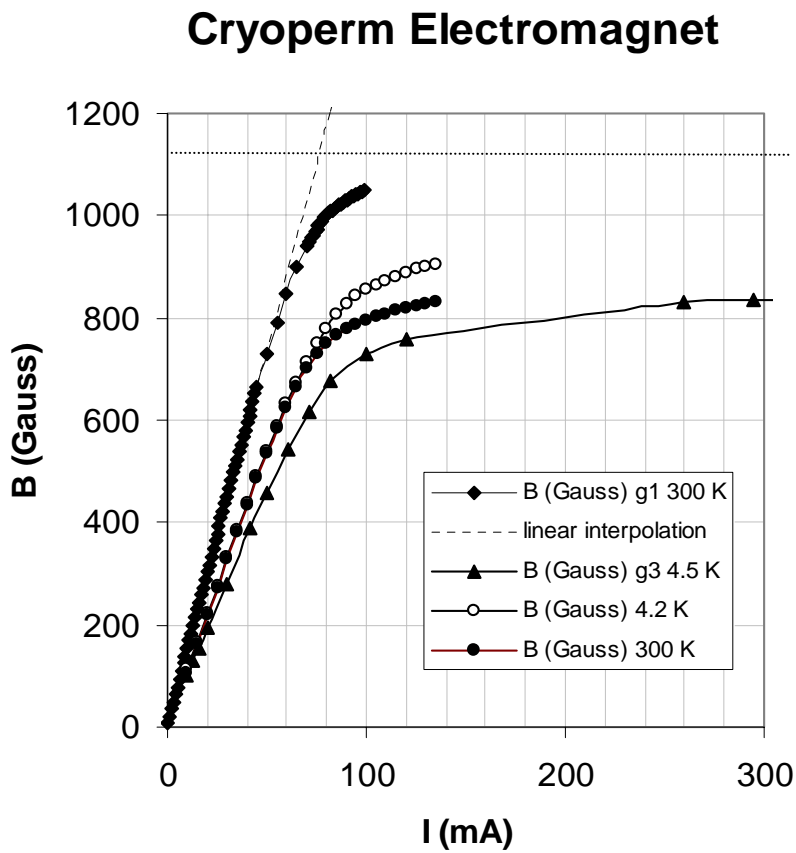
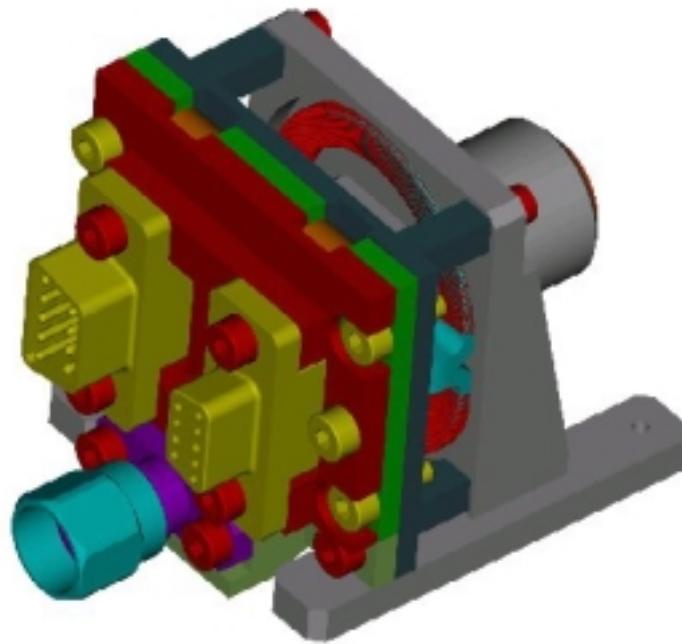


Figure 9. Magnetic field vs. current measured on the Band 1 prototype cryoperm electromagnet, with 1100 turns, at ambient and LHe temperatures and for three gap values : the permeability decreases as g is increased. The final magnet will have a gap of 1 mm $< g_1$.

(a)



(b)

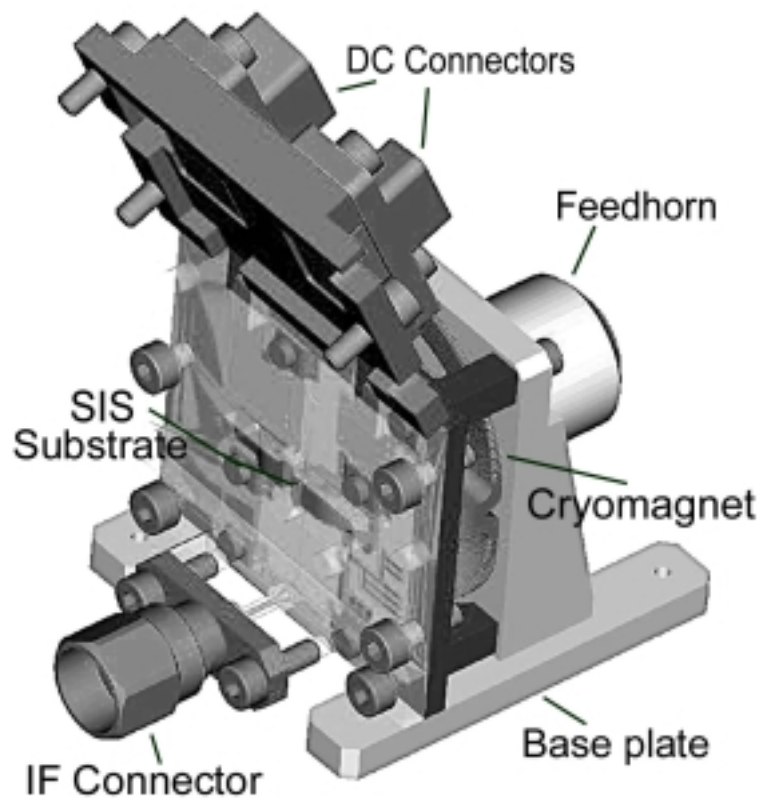


Figure 10. 3D Autocad view of the DM mixer for Band 1: (a) closed; (b) open.

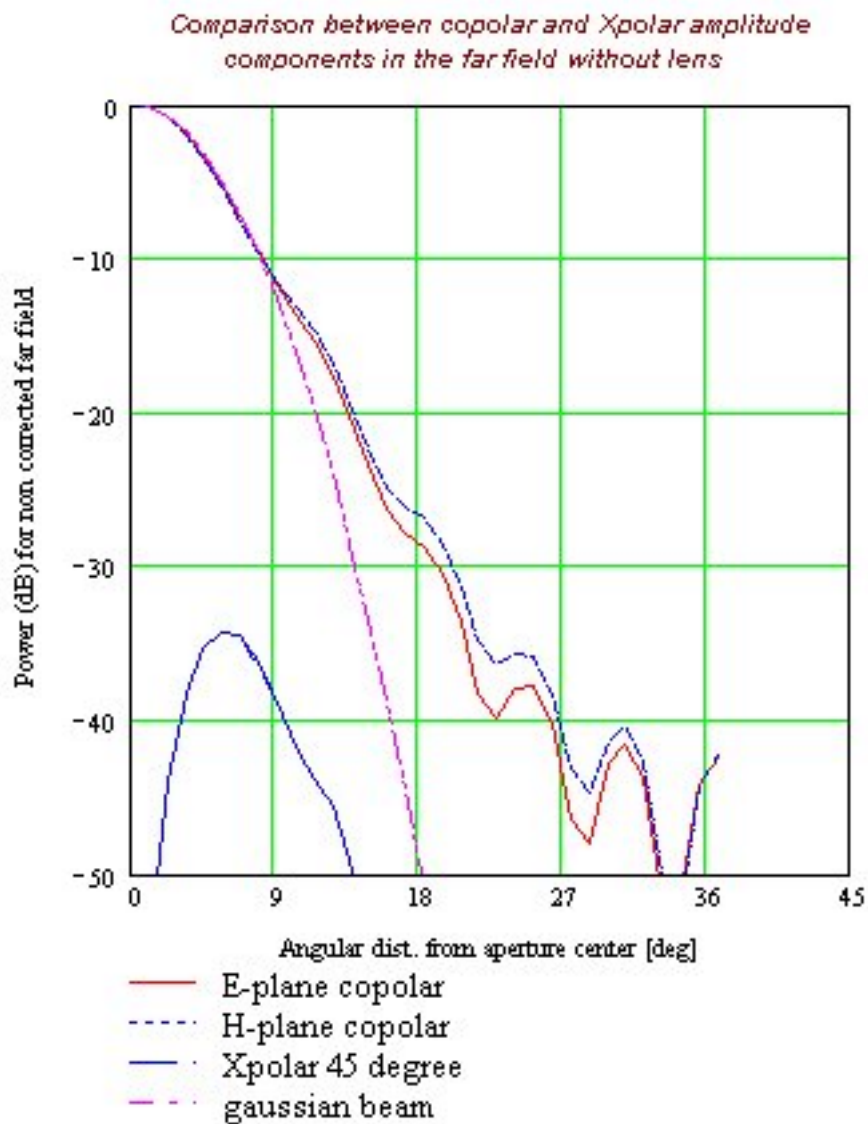


Figure 11. Calculated beam pattern and cross-polarization level for Band 1 (the same horn profile has been adopted for all waveguide mixer bands).

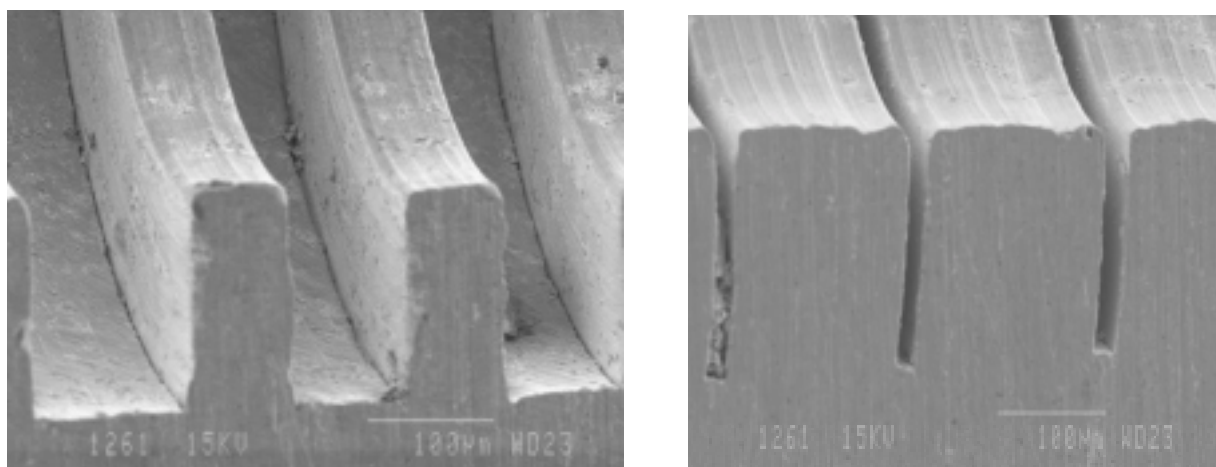


Figure 12. EBM inspection of the corrugated gold parts of two prototype feedhorns with 70 μm (left) and 20 μm (right) wide corrugations.